A Two-Step Preparation of Silica-Supported Calcium-Molybdenum Catalysts

Karen Malka*,† and Jean-Michel Tatibouët†,[1]

*Laboratoire de Réactivité de Surface, URA CNRS 1106, Université Pierre et Marie Curie, 4, place Jussieu, 75252 Paris cedex 05, France; and †Laboratoire de Catalyse en Chimie Organique, UMR CNRS 6503, Ecole Supérieure d'Ingénieurs de Poitiers, 40, avenue du Recteur Pineau, 86022 Poitiers cedex, France

In order to investigate the role of Ca content on the nature of the active phase of silica supported molybdenum based catalysts, we have prepared by a two-step procedure, a series of catalysts containing the same amount of molybdenum (1, 2, and 10 Mo wt%) but with variable Ca/Mo atomic ratios, ranging from 0 to 4. We have shown by XRD, Raman spectroscopy, and methanol oxidation reaction, that molybdenum species react with previously deposited Ca, leading to the formation, for Ca/Mo atomic ratios lower than one, of two kinds of calcium molybdate species on the silica support: (a) crystallized $CaMoO_4$ particles originating from calcium phase large clusters; (b) highly dispersed $CaMoO_x$ species formed from highly dispersed Ca^{II} ions. These latter species have been found catalytically very active in methanol oxidation for the selective formation of methyl formate, whereas supported $CaMoO_4$ particles behave as bulk $CaMoO_4$ (low catalytic activity and carbon oxide formation), as observed for Ca/Mo atomic ratios higher than one, where only crystallized $CaMoO_4$ particles are formed.   © 1998 Academic Press

1. INTRODUCTION

Control of the dispersion of the active phase on a support is a constant preoccupation in the supported catalysts preparation, and particularly in silica supported molybdenum oxide (1–9). The catalysts are generally prepared by contacting with the support a solution containing the precursor of the active phase. After solvent elimination, the precursor species remaining on the support surface can develop two main kinds of interactions:

—interaction between precursor species and support
—interaction between precursor species themselves.

It is generally postulated that if precursor species are in stronger interaction with support than with themselves, the resulting dispersion of precursor species will be high. By contrast, if the interprecursor species interaction is stronger than the precursor species–support interaction, a poor dispersion of the precursor species will be attained with formation of aggregates (10, 11).

In the supported oxide preparation, the precursor transformation into an active catalyst is generally performed by thermal treatment under air or pure oxygen. During this transformation, several phenomena can occur, the elemental constituents of the active phase being able to spread out on the support surface, to react with the support, or to aggregate into crystallized tridimensional particles (12).

We can expect that the same previous concept can be used to explain the various dispersion observed, the nature of these interactions being, however, different: they are mainly electrostatic in the catalyst precursor formation while they are iono-covalent for the active catalyst (12).

In this point of view, molybdenum oxide supported on silica can be considered as a typical example of potentially poorly dispersed catalyst, since molybdenum oxide, i.e. MoO_3, and silica are considered to have an acidic character, and then not to undergo strong interaction between active phase and support. Moreover, it has been shown that molybdenum oxide species can spread out on the support upon calcination (13, 14).

According to Wachs *et al.* on the possibility of reaction of alkaline or alkaline earth silica impurities with molybdenum species (10, 15), and considering these impurities possess a strong basic character able to develop strong interactions both with silica and molybdenum oxide, we have checked if highly dispersed silica supported molybdenum oxide may be prepared by a two-step impregnation–calcination procedure. The first step consists in dispersing the added alkaline cation on silica and the second step in depositing the molybdenum oxide.

In this work, we have investigated the Mo-Ca-O/SiO_2 system, prepared according to the preceding concepts of the two-step procedure. We can then expect that by varying the Ca/Mo atomic ratio, if the Ca cations are well-dispersed and act as germination sites towards molybdenum oxide, it will be possible to control the nuclearity of molybdenum

[1] Corresponding author.

oxide clusters growing around this Ca center, and then the oxide active phase dispersion.

2. EXPERIMENTAL SECTION

2.1. Sample Preparation

The Spherosil XOA 400 silica, supplied by Rhône Poulenc (France), was used as support. Before uses, silica was thoroughly washed with nitric acid ($1M$) in order to eliminate most of the impurities. After washing, silica has a surface area of 500 $m^2 \cdot g^{-1}$, a porous volume of 1.14 mL $\cdot$ g^{-1}, and a mean pore diameter of 95 Å. Chemical analysis reveals the presence of 4 ppm of Ca and 60 ppm of Na.

The samples containing calcium and molybdenum oxide, labelled as Mo/Ca/SiO₂, are prepared by two consecutive incipient wetness-calcination procedures to deposit in the first step the calcium cations and in second step the molybdenum oxide.

The first impregnation was performed with an aqueous solution (1.5 mL per g of silica) of calcium nitrate $Ca(NO_3)_2$, 4 H_2O (Prolabo, 97%). The solvent excess was evaporated in a water bath at 80°C under a manual stirring. The solid obtained was dried in an oven at the same temperature overnight, then calcined 2 hr in a flow reactor under an oxygen stream (100 mL $\cdot$ min^{-1}) at 450°C (heating rate: 7.5°C $\cdot$ min^{-1}) to obtain the doped support, labelled as Ca/SiO₂.

For the second step, the calcined Ca/SiO₂ samples were impregnated with an aqueous solution (1.5 mL per g of silica) of ammonium heptamolybdate $(NH_4)_6Mo_7O_{24}$, 4 H_2O (Prolabo, 99%) with a concentration of 12.3, 24.5, and 122.7 g $\cdot$ L^{-1} to obtain samples (Mo/Ca/SiO₂) containing Mo 1 wt% (labelled as 1Mo/Ca/SiO₂), 2 wt% (labelled as 2Mo/Ca/SiO₂), and 10 wt% (labelled as 10Mo/Ca/SiO₂), respectively. The solvent excess was evaporated in a water bath at 80°C under a manual stirring, followed by drying in an oven at the same temperature overnight. After cooling, the samples were directly put in a dessicator. Before any experiment, all the samples were standardized by 1 h calcination under oxygen stream at 300°C followed by 2 h at 450°C without any further air contact.

Two additional samples containing Mo 2 wt%, with the atomic ratio Ca/Mo = 1, have been differently prepared. The first one was prepared by inverting the two steps of the standard procedure: the molybdenum precursor was first impregnated according to the procedure used for the standard samples, followed by Ca impregnation and calcination (450°C, 2 h). This sample is labelled as Ca/2Mo/SiO₂. The other sample was prepared by the same procedure as standard samples for the first step (Ca deposit), but the second step was divided in two consecutive steps, identical to the standard procedure, with only 1 Mo wt% per step. This sample is labelled as 1Mo/1Mo/Ca/SiO₂.

TABLE 1

Ca Amount (Ca wt%) on the Samples Containing 1, 2, and 10 Mo wt% at Different Ca/Mo Atomic Ratios

Ca/Mo (at. ratio)	0.001	0.01	0.1	0.2	0.5	1	2	4
1/Mo/Ca/SiO₂	—	—	—	0.08	—	0.42	0.83	—
2Mo/Ca/SiO₂	8×10^{-4}	0.008	0.08	—	0.42	0.83	1.7	3.3
10/Mo/Ca/SiO₂	—	—	0.42	—	—	4.2	—	—

For each of series, the molybdenum amount was kept constant, either 1, 2, or 10 wt%, whereas the Ca amount was changed in order to ensure various Ca/Mo atomic ratio, in the range 0–4 (Table 1).

For example, the sample labelled as 2Mo/Ca/SiO₂ (Ca/Mo = 1) corresponds to 2 wt% Mo on silica doped by Ca with an atomic ratio Ca/Mo = 1, i.e. 0.83 wt% Ca on silica. It was prepared by following the standard procedure (Ca is first deposited on SiO₂ and then the molybdenum precursor is impregnated after calcination), while for the sample labelled as Ca/2Mo/SiO₂ (Ca/Mo = 1) which contains the same amounts of Ca and Mo, the two preparation steps were inverted.

Unsupported orthorhombic α-MoO₃ was prepared by precipitation of an aqueous solution of ammonium heptamolybdate (182 g $\cdot$ L^{-1}), heated in a water bath at 80°C, by adding a concentrated solution of nitric acid. After washing with distilled water, the precipitate was calcined 5 h at 400°C (16). The orthorhombic structure of α-MoO₃ was checked by X-ray diffraction (X-ray diffractometer Siemens D-500).

SiO₂, α-MoO₃, and CaMoO₄ (Johnson Matthey, Alfa Products, 96%) were used as reference samples.

2.2. Techniques

Raman spectroscopy. The Raman spectra of 1 and 2 Mo wt% containing samples, were recorded at room temperature in ambient air on a Jobin–Yvon T 6400 spectrometer, using the 514.5 nm radiation of a Ar$^+$ laser.

The Raman spectra of 10Mo/Ca/SiO₂ samples after calcination were recorded *in situ*, without further ambient air contact, at room temperature on a modular Dilor XY spectrometer using Ar$^+$ laser at 514.5 nm (Spectra-Physics Model 165). On both spectrometers, Raman spectra were obtained through a microscope which allows us to analyze a single grain of silica. For a same sample, the Raman analysis was performed on different grains of a catalyst in order to check the homogeneity and the nature of the surface oxide phase. The spectral resolution was estimated to be 5 cm^{-1}.

X-ray diffraction (XRD). A Siemens D500 diffractometer was used to perform X-ray diffraction on 1Mo/Ca/SiO₂ and 2Mo/Ca/SiO₂ samples for various Ca/Mo atomic ratios in order to check the presence of crystallized oxide phase on silica support. The mean particles size

Ca/Mo (at. ratio)	0.1	0.2	0.5	1	2	4
1Mo/Ca/SiO$_2$	—	245	—	330	215	—
1Mo/1Mo/Ca/SiO$_2$	—	—	—	235	—	—
2Mo/Ca/SiO$_2$	345	—	270	250	200	160

(Table 2) was estimated from the profile of the main diffraction line (112) of CaMoO$_4$, according to the Scherrer equation ($2\theta = 28.8°$; $d_{(112)} = 3.10$ Å).

Methanol oxidation. Methanol oxidation was used as a test reaction in a continuous-flow isothermal fixed-bed reactor (17) operating at atmospheric pressure. The composition of the reactant feed CH$_3$OH/O$_2$/He was in the molar ratio 7.1/15.5/77.4, which corresponds to a methanol partial pressure of 54 Torr. The reactant mixture was obtained by flowing an O$_2$/He gas mixture through a methanol saturator maintained at 10°C. The overall flow rate and the catalyst weight were adjusted in order to secure a moderate methanol conversion, not exceeding 10%. Catalytic measurements were performed at steady state, usually about 70 min after the reactant feed was contacted with the catalyst.

On-line computerized gas chromatographic analysis was used to determine the feed composition before and after passing through the catalytic reactor. The reaction rates are expressed as the methanol consumption for the formation of a given product per hour and per gram of catalyst. The selectivities are calculated as the rate ratio between a product formation and the total methanol consumption (17).

3. RESULTS

3.1. Raman Spectroscopy

The Raman spectra of Mo 2 wt% samples with various Ca/Mo ratios are shown in Figs. 1 and 2, and 10 Mo wt% in Fig. 3. On all the samples, broad Raman features of silica support are visible at 980, 800, 600, and 480 cm^{-1} (10, 18–20). The Raman bands characteristic of crystallized α-MoO$_3$ are never detected, even for the Ca free sample containing 10 wt% Mo.

2Mo/Ca/SiO$_2$ samples. On the Raman spectrum of the sample without calcium (Ca/Mo = 0, Figs. 1a and 2a), in addition to silica bands, only a sharp Raman band at 980 cm^{-1} with a shoulder at 960 cm^{-1} and a small band at 840 cm^{-1} are present. These bands could be assigned to the presence on the silica surface of silicomolybdic acid, as revealed by a sharp band at 980 cm^{-1} with a shoulder at 960 cm^{-1} (2, 3, 21). This species results in the transformation from air moisture of the surface molybdate species (21). However, we cannot exclude the presence of hydrated polymolybdate

species (22–24), which exhibit Raman bands in the same region (955–960 cm^{-1}).

On all the calcium containing samples, the Raman features of CaMoO$_4$ are clearly visible by intense bands at 878, 847, 794, 390, 321, 203, 141, and 110 cm^{-1} (10, 21). For Ca/Mo = 0.5 (Fig. 1b), a small Raman feature at 980–940 cm^{-1} shows that in addition of CaMoO$_4$, hydrated molybdate species are also present on the silica surface (10, 13), a small part being transformed into silicomolybdic acid (21). The silica feature at 980 cm^{-1} whose intensity is roughly proportional to the silica Raman feature visible at 480 cm^{-1} could contribute to the feature of molybdate species, but the low intensity of the silica band at 480 cm^{-1} in this spectrum indicates that its contribution is negligible.

For Ca/Mo = 1 (Fig. 1d), only Raman features of CaMoO$_4$ are unambiguously visible. However, the Raman feature at 980 cm^{-1}, which is unsymmetrical, suggests that a small amount of molybdate species is still present on the silica surface as hydrated molybdate species.

For Ca/Mo ratios of 2 and 4 (Figs. 1e and 1f), a new Raman feature appears at 1050 cm^{-1} which could be likely
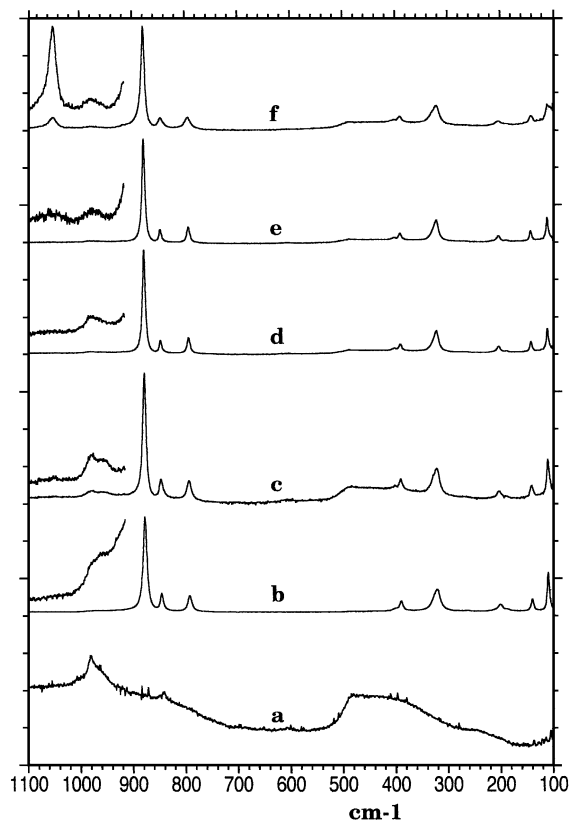

FIG. 1. Raman spectra of 1Mo/1Mo/Ca/SiO$_2$ and 2Mo/Ca/SiO$_2$ samples with various atomic ratios. Enlarged view of the spectra in the range 1100–915 cm^{-1} have been normalized on the basis of the same intensity of the silica Raman feature at 480 cm^{-1}: (a) Ca/Mo = 0; (b) Ca/Mo = 0.5; (c) 1Mo/1Mo/Ca/SiO$_2$, Ca/Mo = 1; (d) Ca/Mo = 1; (e) Ca/Mo = 2; (f) Ca/Mo = 4.
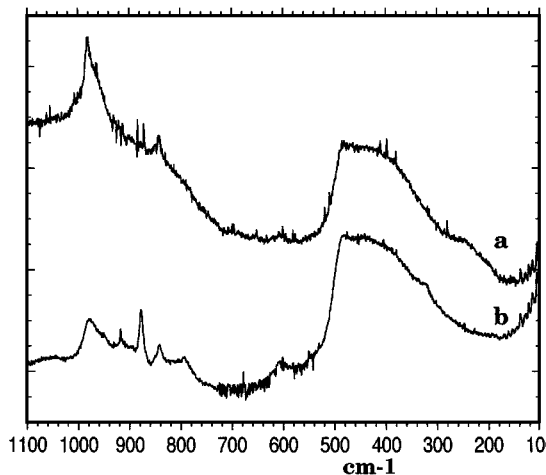
FIG. 2. Raman spectra of 2Mo/SiO₂ (a); and Ca/2Mo/SiO₂ (b).

assigned to the presence of Ca carbonate species resulting from the reaction of carbon dioxide from ambient air on calcium oxide or hydroxide during the catalysts preparation (25, 26).

1Mo/1Mo/Ca/SiO₂. The Raman spectrum of this sample (Fig. 1c) shows, in addition of the features of CaMoO₄, two broad bands at 980 and 955 cm^{-1} that are characteristic of molybdate species uncombined with Ca ions.

Ca/2Mo/SiO₂ sample. This spectrum (Fig. 2b) is close to that of 2Mo/SiO₂, with only a weak Raman signal at 880 cm^{-1} corresponding to CaMoO₄, indicating that owing to the procedure used for the preparation, molybdenum oxide and calcium cations do not react together, suggesting that Ca ions are randomly deposited on the 2Mo/SiO₂ support.

10Mo/Ca/SiO₂ samples. These Raman spectra (Fig. 3) were performed on the calcined samples, kept in a sealed tube, without further air or moisture exposure.

The behavior of 10Mo/Ca/SiO₂ samples upon increasing the Ca content is about the same as for the 2Mo/Ca/SiO₂ samples. For Ca/Mo = 0, only dehydrated polymolybdate species (22–24) are visible (Raman bands at 996 and 967 cm^{-1}). By increasing the Ca content, the calcium molybdate Raman features appear in addition to dehydrated polymolybdate species. At Ca/Mo = 1, only the Raman bands characteristic of calcium molybdate are detected. Those of crystallized α-MoO₃ are never detected on these samples.

3.2. X-Ray Diffraction

The diffraction patterns of 2Mo/Ca/SiO₂ samples with various Ca/Mo ratio (Ca/Mo = 0, 0.1, 0.5, 1, 2, and 4) are shown on Fig. 4. As already probed by Raman spectroscopy, only the diffraction lines assignable to crystallized CaMoO₄ are visible on Ca containing samples. On Ca-free samples (2Mo/SiO₂ and 10Mo/SiO₂) the diffraction lines of crys-

tallized α-MoO₃ are not detected. The mean particles size of crystallized CaMoO₄, estimated from the profile of the diffraction line (112) of CaMoO₄ are presented in Table 2. We should note that on the 2Mo/Ca/SiO₂ samples, the particles size decreases when the Ca/Mo ratio increases.

3.3. Methanol Oxidation

SiO₂ and Ca/SiO₂ supports. Activities and selectivities obtained on pure SiO₂ and doped supports Ca/SiO₂ resulting from the first step of the preparation procedure, i.e. before the Mo impregnation, are reported in Table 3.

We should note that the catalytic activity of pure spherosil XOA 400 silica is unusually high, compared to that measured on other supports such as SiO₂, TiO₂, and Al₂O₃ (27–30).

For the very low Ca loading (until 80 ppm), the influence of the Ca amount seems negligible, the catalytic behavior being similar to that of pure silica. When the Ca loading increases from 80 ppm to 0.4 wt% (4000 ppm), a dramatic decrease in both methyl formate and dimethyl ether formation rates occurs, whereas the formation rates
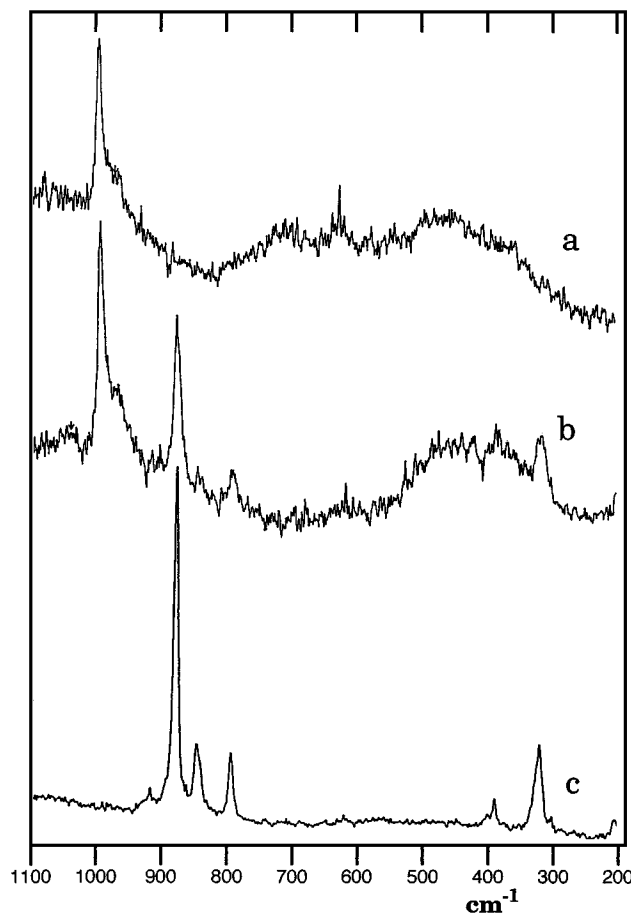

FIG. 3. Raman spectra of 10Mo/Ca/SiO₂ samples with various Ca/Mo atomic ratios: (a) Ca/Mo = 0; (b) Ca/Mo = 0.1; (c) Ca/Mo = 1.
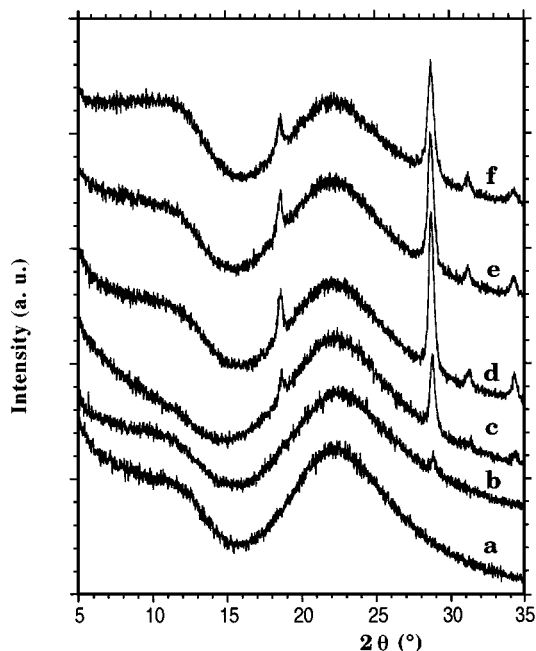
FIG. 4. X-ray diffraction patterns of 2Mo/Ca/SiO$_2$ samples with various Ca/Mo atomic ratios (Cu Kα radiation, $\lambda = 1.5406$ Å): (a) Ca/Mo = 0; (b) Ca/Mo = 0.1; (c) Ca/Mo = 0.5; (d) Ca/Mo = 1; (e) Ca/Mo = 2; (f) Ca/Mo = 4.

of other reaction products remain almost constant. For a Ca amount higher than 800 ppm (0.08 wt%), the catalytic activity of the Ca/SiO$_2$ samples appears to be stabilized at a value about three times lower than those of pure silica (Table 3 and Fig. 5). However, the carbon oxide selectivity increases continuously at the expense of the methyl formate one.

Mo/Ca/SiO$_2$ samples. Activities and selectivities of the samples containing 1, 2, and 10 Mo wt% with various Ca/Mo atomic ratio, and of the reference samples CaMoO$_4$ and α-MoO$_3$ are reported in Tables 4 to 6.

TABLE 3

Selectivities and Overall Reaction Rate in Methanol Oxidation on SiO$_2$ and Ca/SiO$_2$ (Weight = 50 mg, WHSV = 10.5 h^{-1}) at 70 min of Reaction at 260°C, CH$_3$OH/O$_2$/He = 7.7/16.3/76.0 mol%

	SiO$_2$[a]	Ca/SiO$_2$					
Ca (wt%)	0	8.10^{-4}	0.008	0.08	0.4	0.8	4.2
CH$_2$O (%)	10	9	8	15	33	30	27
HCOOCH$_3$ (%)	75	75	74	58	15	12	3
(CH$_3$O)$_2$CH$_2$ (%)	<1	3	4	8	15	16	11
CH$_3$OCH$_3$ (%)	<1	<1	<1	<1	<1	<1	<1
CO$_x$ (%)	14	12	13	18	36	41	58
Overall reaction rate (mmol/h/g)	11.2	12.1	10.5	5.7	3.0	2.7	4.9

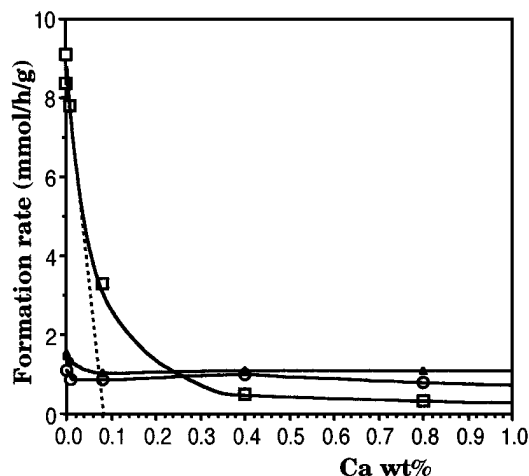[a] Pure SiO$_2$ contains 4 ppm Ca and 60 ppm of Na.

FIG. 5. Methanol oxidation catalytic behavior of Ca/SiO$_2$ samples: □, HCOOCH$_3$ (mmol/h/g); ○, CH$_2$O (mmol/h/g); ▲, CO$_x$ (mmol/h/g).

1Mo/Ca/SiO$_2$ and 2Mo/Ca/SiO$_2$ samples. As already observed for the Ca/SiO$_2$ series, the catalytic behavior of the samples 2Mo/Ca/SiO$_2$ (Table 5) does not change significantly until a Ca/Mo ratio of 0.01 (Ca = 80 ppm). When the Ca/Mo ratio increases to 0.1 (Ca = 800 ppm), a marked increase in the methyl formate formation rate and a decrease in the methylal formation rate are observable (Tables 4 and 5). By increasing the Ca/Mo ratio to 1 (0.8 wt% Ca), the methyl formate formation reaches a plateau with a selectivity as high as 89% at 240°C (Table 4).

By increasing the Ca/Mo ratio to values exceeding 1, a dramatic change in the catalytic behavior (Fig. 6) occurs as shown by an important decrease in the reaction rate and in the methyl formate selectivity. Simultaneously we observe an important increase in the carbon oxide selectivity (Tables 4 and 5), the catalytic behavior being close to those of unsupported CaMoO$_4$ (Table 6).

The 1Mo/Ca/SiO$_2$ samples follow a similar behavior (Table 4) but the decrease in the methyl formate formation rate is already observed at a Ca/Mo ratio of 1.

10Mo/Ca/SiO$_2$ samples. The catalytic behavior (Table 6) of these samples exhibits a continuous change with the Ca/Mo ratio. All the formation rates decrease when the Ca/Mo ratio increases, showing a strong inhibiting effect of Ca on the reaction rate. The methylal and dimethyl ether selectivities decrease continuously when the Ca/Mo ratio increases, whereas the methyl formate and formaldehyde selectivities pass through an extremum (maximum for HCOOCH$_3$, minimum for CH$_2$O) for a Ca/Mo ratio of 0.1 (Ca = 0.43 wt%).

4. INTERPRETATION AND DISCUSSION

SiO$_2$ and Ca/SiO$_2$ supports. Pure silica XOA 400, exhibits an unusually high catalytic activity in methanol

TABLE 4

Selectivities and Overall Reaction Rate in Methanol Oxidation for Samples Containing 2 and 1Mo wt%

Ca/Mo (at. ratio)	2Mo/Ca/SiO$_2$				Ca/2Mo/SiO$_2$	1Mo/1Mo/ Ca/SiO$_2$	1Mo/Ca/SiO$_2$			
	0	0.1	0.5	1	1	1	0	0.2	1	2
S CH$_2$O%	18	13	13	7	15	11	20	12	36	23
S HCOOCH$_3$%	68	81	81	89	80	85	68	81	35	62
S (CH$_3$O)$_2$CH$_2$%	8	3	3	1	2	1	6	4	0	0
S CH$_3$OCH$_3$%	4	1	1	1	1	1	4	1	1	0
S CO$_x$%	2	2	2	2	2	2	2	2	28	15
Overall reaction rate (mmol/h/g)	2.3	5.1	5.3	8.0	6.9	13.0	2.4	4.5	1.7	1.2

Note. T$_R$ = 240°C; CH$_3$OH/O$_2$/He = 7.1/15.5/77.4 mol%.

oxidation at 260°C (Table 3), characterized by a high selectivity in the methyl formate formation (75%). This behavior reveals the presence of catalytic active sites on this silica surface, whose nature remains unclear (31). Nevertheless, the high methyl formate selectivity obtained in methanol oxidation on pure silica has already been reported (30), suggesting that these sites are not specific of our silica support, but are only in higher amounts than on conventional silica and are able to perform redox reactions.

By adding increasing amounts of calcium cations on the silica surface, a strong inhibiting effect on the methyl formate formation rate (and to a lower extent on the dimethyl ether formation rate) is observed, whereas the formation rates of other reaction products remain almost constant (Fig. 5), showing that silica-active sites are poisoned by Ca ions. A rough determination of the amount of these sites $(0.2–0.3 \times 10^{17}$ sites per m^2) can be deduced from Fig. 5 by extrapolating to zero the straight part of the curve describing the variation of the methyl formate formation rate versus the Ca content.

For the highest Ca loading (4.2 Ca wt%), the increase in the overall reaction rate could be due to the presence of a clusterized calcium phase on the silica surface as shown

further on the Raman spectra of 2Mo/Ca/SiO$_2$ (Figs. 1e and 1f) by the band at 1050 cm^{-1}. This calcium phase could result from the transformation of calcium oxide species (formed by calcium nitrate decomposition) into calcium hydroxide species by air moisture exposure or during the molybdenum aqueous impregnation (CaO + H$_2$O → Ca(OH)$_2$). Then, the fast reaction of carbon dioxide that comes from ambient air on the calcium hydroxide species leads to the formation of hydrogenocarbonate species. The final calcination transforms the hydrogenocarbonate species into the stable calcium carbonate species (Ca(OH)$_2$ + 2CO$_2$ → Ca(HCO$_3$)$_2$ → CaCO$_3$ + CO$_2$ + H$_2$O) observed by Raman spectroscopy, the calcination temperature (450°C) being about 150°C below the temperature at which the calcium carbonate decomposition starts, as observed by thermal analysis.

We can conclude that the first step of our preparation of silica-supported molybdenum oxide (calcium deposit) leads to a deep modification of the surface properties of the support.

1Mo/Ca/SiO$_2$ and 2Mo/Ca/SiO$_2$ samples. As expected, the catalytic behavior of samples with a Ca/Mo ratio higher

TABLE 5

Selectivities and Overall Reaction Rate in Methanol Oxidation for 2Mo/Ca/SiO$_2$ Samples

Ca/Mo (at. ratio)	2Mo/Ca/SiO$_2$							
	0	0.001	0.01	0.1	0.5	1	2	4
S CH$_2$O (%)	23	23	29	19	11	8	38	30
S HCOOCH$_3$ (%)	59	66	60	77	85	86	23	10
S (CH$_3$O)$_2$CH$_2$ (%)	11	8	7	1	1	1	0	0
S CH$_3$OCH$_3$ (%)	4	2	1	<1	<1	<1	1	<1
S CO$_x$ (%)	3	2	2	3	3	5	38	60
Overall reaction rate (mmol/h/g)	3.3	4.9	4.9	17.8	18.4	22.4	0.6	1.9

Note. T$_R$ = 260°C; CH$_3$OH/O$_2$/He = 7.1/16.4/76.5 mol%.

TABLE 6

Selectivities and Overall Reaction Rate in Methanol Oxidation for 10Mo/Ca/SiO$_2$ Samples and Unsupported CaMoO$_4$ and α-MoO$_3$

Ca/Mo (at. ratio)	10Mo/Ca/SiO$_2$			CaMoO$_4$	MoO$_3$
	0	0.1	1	—	—
S CH$_2$O (%)	51	37	50	48	52
S HCOOCH$_3$ (%)	13	35	32	4	0
S (CH$_3$O)$_2$CH$_2$ (%)	25	21	9	3	25
S CH$_3$OCH$_3$ (%)	11	7	3	0	23
S CO$_x$ (%)	0	0	5	45	0
Overall reaction rate (mmol/h/g)	7.2	5.2	1.5	1.1	3.4

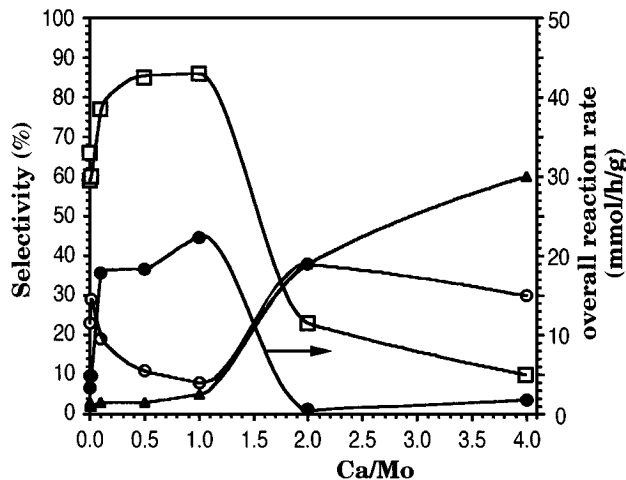*Note.* T$_R$ = 260°C; CH$_3$OH/O$_2$/He = 7.7/16.3/76.0 mol%.

FIG. 6. Methanol oxidation catalytic behavior of 2Mo/Ca/SiO$_2$ samples: □, HCOOCH$_3$ (%); ○, CH$_2$O (%); ▲, CO$_x$ (%); ●, overall reaction rate (mmol/h/g).

than 1, where only the CaMoO$_4$ phase is detected by Raman spectroscopy, is close to that of unsupported CaMoO$_4$. This behavior is characterized by a high selectivity in the carbon oxide formation and a moderate or low selectivity in the methyl formate formation. It also shows that the crystallized CaMoO$_4$ phase is unable to selectively form methyl formate. According to previous studies performed on ultra-dispersed Mo/SiO$_2$ prepared by MoCl$_5$ grafting (8, 18, 32), this product (HCOOCH$_3$) is selectively formed on highly dispersed Mo species and can be regarded as a dispersion probe: the higher the methyl formate formation, the higher the dispersion of the active phase (8, 18, 33). We should then postulate the existence of such species to explain the catalytic behavior observed on the Mo/Ca/SiO$_2$ samples. However, the polymolybdate species or the silicomolybdic acid detected by Raman spectroscopy cannot be taken into account, since when the Ca/Mo ratio increases from 0 to 1 the amount of these species should decrease due to the formation of crystallized CaMoO$_4$ (the Mo content is constant). If these species are responsible of the HCOOCH$_3$ formation, a decrease in the formation rate should occur, due to the decrease in the amount of active sites. An opposite trend is experimentally observed, i.e. an increase in the formation rate of HCOOCH$_3$ with the Ca/Mo atomic ratio, suggesting that these species are not involved in the HCOOCH$_3$ formation mechanism. We propose that the species which selectively catalyze the methyl formate formation are directly correlated with the presence of Ca. We can then postulate that Ca ions are present in two different forms on SiO$_2$ surface as highly dispersed Ca^{II} ions and as large amorphous clusters of a calcium phase (hydroxide or carbonate), even for a low Ca amount. When molybdenum is added, the formation of crystallized CaMoO$_4$ particles from the calcium phase clusters is then more thermodynam-

ically favoured than the formation of the highly dispersed CaMoO$_x$ species (bulk energy stabilization), explaining the presence of crystallized CaMoO$_4$, detected by Raman spectroscopy and XRD for Ca/Mo ratio as low as 0.1. For the Ca/Mo ratios less than 1, the molybdenum excess, in regard to the CaMoO$_4$ formation, allows us to form the highly dispersed CaMoO$_x$ species, expected to be responsible to the selective formation of methyl formate. When the amount of Ca on the silica surface increases, the quantity of the highly dispersed Ca^{II} ions should increase as well as the amount of the calcium phase amorphous clusters, but the molybdenum amount being constant, the molybdenum which does not take part in the crystallized CaMoO$_4$ formation and is able to form the CaMoO$_x$ species with these highly dispersed Ca^{II} ions decreases. A compensation effect should occur, leading to only a slight increase in the quantity of the highly dispersed CaMoO$_x$ species, as revealed by only a small increase in the rate of methyl formate formation (Tables 4 and 5).

Formally, if all the Ca ions are accessible to Mo species, for a Ca/Mo ratio equal to one or only slightly higher, the catalytic behavior should be that of unsupported CaMoO$_4$, as observed with the 1Mo/Ca/SiO$_2$ (Ca/Mo = 1) sample (Table 4). This behavior strongly suggests that the highly dispersed CaMoO$_x$ species represent only a minor part of the total amount of calcium molybdate species and then are catalytically very active for the methanol to methyl formate oxidation.

When the Ca/Mo ratio is higher than 1, all the molybdenum cations can react with the calcium phase amorphous clusters, leading to the formation of only crystallized CaMoO$_4$ particles whose size decreases when the Ca/Mo ratio increases.

As shown by Raman spectroscopy and by the catalytic reaction, the 1Mo/1Mo/Ca/SiO$_2$ sample behaves similarly to the 2Mo/Ca/SiO$_2$ samples (Ca/Mo = 0.5 or 1), whereas the Ca/2Mo/SiO$_2$ sample is close to the calcium-free sample 2Mo/SiO$_2$. This observation means that molybdenum species can react easily with calcium deposits during the calcination procedure, whereas the calcium species are not able to react with previously deposited molybdenum species. This particular behavior could be due to the respective surface mobility of these different species upon calcination conditions and could reflect the nature of their respective interaction with the silica surface: the stronger the interaction, the lower the mobility. We can then conclude that, as expected, the Ca ions develop a stronger interaction with the silica surface than the molybdenum species.

10Mo/Ca/SiO$_2$ samples. For the calcium-free sample, we observed a low methyl formate selectivity (13%) suggesting a low molybdate phase dispersion, as expected if we consider that polymolybdate species grow on silica reactive sites. The higher nuclearity of these species than on 2Mo/Ca/SiO$_2$ samples is also clearly evidenced by a

higher methylal formation rate on 10 Mo wt% sample (1.8 mmol/h/g for 10 Mo wt%, instead of 0.3 mmol/h/g for 2 Mo wt%), since the methylal which needs three methanol molecules to be formed is favoured by the presence of methanol adsorption sites in close vicinity (17, 34, 35). The higher formaldehyde selectivity on the 10 Mo wt% sample (51% vs 23% on 2 Mo wt%) confirms its low active phase dispersion (17, 18, 36).

When Ca modifies the silica support, the silica reactive sites are first used as Ca adsorption sites, but the amount (0.42 wt%) needed to attain a Ca/Mo ratio of 0.1, for example, exceeds largely the number of these sites, estimated to be ≈ 0.08 Ca wt% (Fig. 5). A high dispersion ought to be obtained, leading to a high methyl formate selectivity. Unfortunately, despite the fact that the methyl formate selectivity increases, the value is only 35%, suggesting a poor or moderate dispersion. This apparent contradiction could be due to the too high coverage (0.2–0.4 monolayer, depending on the calcul mode) of the silica surface by molybdenum species which favours the aggregate formation.

By increasing the Ca content to obtain a Ca/Mo ratio of 1, only the calcium molybdate species is visible by Raman spectroscopy, but it is poorly dispersed as shown by the low methyl formate selectivity obtained on this sample.

5. CONCLUSION

We have investigated the dispersing role of Ca ions, on a molybdenum-based oxide phase supported on silica. Various amounts of Ca were previously deposited on the silica surface to modify its local properties and then to create preferential adsorption sites toward molybdate species. The supports (modified silica) and catalysts were characterized by Raman spectroscopy, X-ray diffraction, and methanol oxidation used as a catalytic reaction probe. The results show that the calcium ions are preferentially localized on unknown "reactive sites" of the silica surface. In the absence of Ca deposit, these sites constitute anchorage sites for the polymolybdate species obtained after calcination whose nuclearity depends on the Mo amount. After the Ca deposit, a strong interaction exists between the Ca ions and the molybdate species, leading to the formation of two kinds of calcium molybdate species on the silica surface: crystallized CaMoO₄ particles originating from calcium phase clusters and highly dispersed CaMoO$_x$ species which are catalytically very active, these latter species being formed from the highly dispersed Ca^{II} ions. By increasing the Ca/Mo ratio to a value higher than 1, only crystallized CaMoO₄ particles are formed, leading to a dramatic change in the catalytic behavior characterized by an important decrease in the overall reaction rate and in the methyl formate formation, and an increase in the carbon oxide selectivity, the catalytic behavior becoming close to those of unsupported CaMoO₄.

The same behavior is observed for the 10 Mo wt% content samples, but to a lower extent, due to an aggregate formation favoured by an important silica coverage. Nevertheless, whatever the catalyst and the Mo content are, crystallized MoO₃ was never detected.

The formation of large CaMoO₄ particles originating from the calcium phase clusters suggests that, unfortunately, the interaction between the calcium species is stronger than its interaction with the silica surface. This then leads to the formation of calcium phase aggregates. We can then expect to increase the amount of isolated CaMoO$_x$ species by efficiently controlling the dispersion of the calcium ions.

REFERENCES

1. Marcinkowska, K., Rodrigo, S., Kaliaguine, S., and Roberge, P. C., *J. Mol. Cat.* **33**, 189 (1985).
2. Rodrigo, L., Marcinkowska, K., Adnot, A., Roberge, P. C., Kaliaguine, S., Stencel, J. M., Makovsky, L. E., and Diehl, J. R., *J. Phys. Chem.* **90**, 2690 (1986).
3. Stencel, J. M., Diehl, J. R., D'este, J. R., Makovsky, L. E., Rodrigo, L., Marcinkowska, K., Adnot, A., Roberge, P. C., and Kaliaguine, S., *J. Phys. Chem.* **90**, 4739 (1986).
4. Marcinkowska, K., Rodrigo, L., Kaliaguine, S., and Roberge, P. C., *J. Catal.* **97**, 75 (1986).
5. Fricke, R., Hanke, W., and Ohlmann, G., *J. Catal.* **79**, 1 (1983).
6. Iwasawa, Y., "Advances in Catalysis," Vol. 35, p. 265. Academic Press, New York, 1987.
7. Yermakov, Y. I., *Catal. Rev.-Sci. Eng.* **13**, 77 (1976).
8. Che, M., Louis, C., and Tatibouët, J. M., *Polyhedron* **5**, 123 (1986).
9. Che, M., and Louis, C., *J. Phys. Chem.* **91**, 2875 (1987).
10. Williams, C. C., Ekerdt, J. G., Jehng, J. M., Hardcastle, F. D., Turek, A. M., and Wachs, I. E., *J. Phys. Chem.* **95**, 8781 (1991).
11. Wachs, I. E., Deo, G., Kim, D. S., Vuurman, M. A., and Hu, H., *in* "New Frontiers in Catalysis, Proceedings, 10th International Congress on Catalysis, 19–24 July 1992, Budapest, Hungary" (L. Guczi *et al.*, Eds.), p. 543. Elsevier, Amsterdam, 1993.
12. Che, M., *in* "New Frontiers in Catalysis, Proceedings, 10th International Congress on Catalysis, 19–24 July 1992, Budapest, Hungary" (L. Guczi *et al.*, Eds.), p. 31. Elsevier, Amsterdam, 1993.
13. de Boer, M., van Dillen, A. J., Koningsberger, D. C., Geus, J. W., Vuurman, M. A., and Wachs, I. E., *Catal. Lett.* **11**, 227 (1991).
14. Roark, R. D., Kohler, S. D., and Ekerdt, J. G., *Catal. Lett.* **16**, 71 (1992).
15. Bañares, M. A., Spencer, N. D., Jones, M. D., and Wachs, I. E., *J. Catal.* **146**, 204 (1994).
16. Tatibouët, J. M., and Germain, J. E., *C. R. Acad. Sci. Paris* **290 C**, 321 (1980).
17. Tatibouët, J. M., *Appl. Catal. A* **148**, 213 (1997).
18a. Galeener, F. L., and Lucosky, G., *Phys. Rev. Lett.* **37**, 1474 (1976).
18b. Galeener, F. L., and Sen, P. N., *Phys. Rev. B* **17**, 1928 (1978).
18c. Galeener, F. L., *Phys. Rev. B* **19**, 4292 (1979).
18d. Galeener, F. L., and Mikkelsen, J. C., Jr., *Phys. Rev. B* **23**, 5527 (1981).

19. Shibata, N., Horigudhi, M., and Edahiro, T., *J. Non-Crystal. Solids* **45**, 115 (1981).
20. Bertoluzza, A., Fagnano, C., Gottardi, V., and Guglielmi, M., *J. Non-Crystal. Solids* **48**, 117 (1982).
21. Rocchiccioli-Deltcheff, C., Amirouche, M., Che, M., Tatibouët, J. M., and Fournier, M., *J. Catal.* **125**, 292 (1990).
22. Hardcastle, F. D., and Wachs, I. E., *J. Raman Spectrosc.* **21**, 683 (1990).
23. Roark, R. D., Kohler, S. D., Ekerdt, J. G., Kim, D. S., and Wachs, I. E., *Catal. Lett.* **16**, 77 (1992).
24. Wachs, I. E., *Catal. Today* **27**, 437 (1996).
25. Anderson, A., *Spectrosc. Lett.* **29**, 819 (1996).
26. Behrens, G., Kuhn, L. T., Ubic, R., and Heuer, A. H., *Spectrosc. Lett.* **28**, 983 (1995).
27. Louis, C., and Che, M., *J. Catal.* **109**, 354 (1988).
28. Kim, D. S., Tatibouët, J. M., and Wachs, I. E., *J. Catal.* **136**, 209 (1992).
29. Cairati, L., and Trifiro, F., *J. Catal.* **80**, 25 (1983).
30. Cheng, W. H., *Catal. Lett.* **36**, 87 (1996).
31. Krylov, O. V., *React. Kinet. Catal. Lett.* **35**, 315 (1987).
32. Louis, C., Che, M., and Bozon-Verduraz, F. J., *Chim. Phys.* **79**, 803 (1982).
33. Louis, C., Che, M., and Anpo, M., *J. Catal.* **141**, 453 (1993).
34. Edwards, J. E., Nicolaidis, J., Cutlip, M. B., and Bennett, C. O., *J. Catal.* **50**, 24 (1977).
35. Ziolkowski, J., *J. Catal.* **84**, 317 (1983).
36. Allison, J. N., and Goddard III, W. A., *J. Catal.* **92**, 127 (1985).